

# Analysis of Waveguides by use of the Time-Domain Finite-Element Method Solved by Preconditioned Iterative Methods

Z. B. Ye D. Z. Ding Z. H. Fan

Department of Communication Engineering

Nanjing University of Science and Technology, Nanjing, 210094, China

Y. Yang

Department of Electronic Engineering

Nanjing University of Aeronautics and Astronautics, Nanjing, 210016, China

*Abstract:* Several preconditioning techniques, such as Jacobi, SSOR and ILU0, are used to accelerate the convergence of iterative methods, such as CG and GMRES, which are used to solve the large system of linear equations resulted from the time-domain finite-element methods (TDFEM). Convergence properties and the time used of these conventional preconditioning techniques are also compared and analyzed. The cylindrical cavity partially filled with dielectric rod and the PML terminated waveguides are simulated. Numerical results show that the ILU0 preconditioned method converges the fastest and costs the smallest time in TDFEM compared with other preconditioning techniques when computing the same number of time steps.

*Keywords:* preconditioning techniques, iterative methods, time-domain finite-element methods (TDFEM), convergence properties

## I. INTRODUCTION

Over the past few years, numerical schemes for simulating electromagnetic transients have grown increasingly popular for their potential to generate wide-band data and model nonlinear materials. The most popular one is the finite-difference time-domain (FDTD) method [1] for transient analysis involving complex inhomogeneous bodies [2-3]. However, this method possesses topological limitation of staircasing [4-6]. In contrast, the finite-element time-domain (TDFEM) can easily handle both complex geometry and inhomogeneous media by using tetrahedral edge elements [7-12].

A variety of TDFEM schemes have been proposed during the past decades [7-22]. These schemes fall into two categories. The first scheme solves the time-dependent Maxwell's equations directly. It yields an explicit finite-difference-like leap-frog, conditionally stable time-marching algorithm [13-16]. The second scheme discretizes the second-order vector wave equation, known as the curl-curl equation, involving one of the field variables from Maxwell's equations [7-11]. It is similar to the traditional frequency-domain finite element method and it can be made unconditionally stable if the Newmark-beta method is used for temporal discretization [8-10].

For the first scheme, two unconditionally stable vector TDFEM methods based on the alternating-direction implicit (ADI) and Crank-Nicolson (CN) schemes to directly solving the first-order Maxwell's equations, which is preferred in some electromagnetic

simulations, have been proposed recently [15-16]. The time step is no longer restricted by the numerical stability, but by the modeling accuracy of the TDFEM algorithm. However, in order to balance both accuracy and efficiency, the time step sometimes is chosen to be no longer than that of the second scheme of TDFEM when simulating the same structure.

For the second scheme, the large system of linear equations resulted from the second-order vector wave equation need to be solved in each time step, the same as the first scheme, which lead to a fully implicit system. Several mass lumping techniques [17-18], which are of a popular approximation to produce diagonal mass matrices in TDFEM in order to obtain explicit schemes without solving the system equation, have been proposed to render the mass matrix diagonal to obviate the need for its inversion. Unfortunately, these lumping techniques often introduce significant errors for not well-shaped mesh elements and they are likely to produce zero or negative diagonal elements, which result in the definite instability [20]. Recently a set of orthogonal vector basis function yielding a diagonal mass matrix for both two-dimensional (2-D) and three-dimensional (3-D) has been constructed [19-20]. It introduces three times more unknowns and the time step size is much smaller than that in the traditional implicit TDFEM scheme. It is also not easy to develop this kind of vector basis function to high order. A new explicit TDFEM method, in which no global system matrix has to be assembled and solved as required in the implicit TDFEM, has been introduced [21-22]. It is fundamentally different from traditional explicit TDFEM formulations. This new method is derived from a recently domain decomposition algorithm by extending domain decomposition to the element level and computes the electric and magnetic fields in a leapfrog fashion while solving the dual-field second-order wave equations. The total number of unknowns is doubled as compared to the traditional implicit TDFEM scheme and it is conditional stable with the stability condition depending on the spatial discretization [22].

The traditional implicit TDFEM scheme can be solved by either direct methods [25-26] or iterative methods. However, the direct methods bring “fill-in,” that is, nonzero entries are created in certain positions where the coefficient matrix originally has zeros. Fill-in is undesirable because it increases both the computing time and the storage requirement. Direct solvers usually suffer from fill-in to an extent that the large problems cannot be solved at a reasonable cost, even on the state-of-the-art parallel machines. Here, we solve the traditional implicit TDFEM scheme by iterative solvers, preconditioned CG [27-34] and GMRES [35-38] methods. Several preconditioning techniques, such as Jacobi, SSOR and ILU0, are used to accelerate the convergence of iterative methods. The preconditioning of the system matrix is the same at each time step, so we could factorize the system matrix before time marching and then reuse the factorization repeatedly at each time step to minimize the total computation. Convergence properties and the time used of these conventional preconditioning techniques will be compared and analyzed.

This paper is organized in the following manner. Section II introduces the traditional implicit TDFEM scheme with perfectly matched layer (PML) and the iterative solvers, as well as the preconditioning techniques. Section III shows the numerical results and discussions. The conclusion is presented in section IV.

## II. THEORY

The uniaxial perfectly matched layer (UPML) is employed to terminate the computational domain. From the Maxwell's equations in the anisotropic material, it is possible to obtain the curl-curl equation as:

$$\nabla \times \frac{1}{\mu} \left( [\Lambda]^{-1} \cdot \nabla \times E \right) - \omega^2 \varepsilon [\Lambda] E = 0 \quad (1)$$

$$\Lambda = \hat{x}\hat{x} \left( \frac{S_y S_z}{S_x} \right) + \hat{y}\hat{y} \left( \frac{S_x S_z}{S_y} \right) + \hat{z}\hat{z} \left( \frac{S_x S_y}{S_z} \right) \quad (2)$$

Where,  $S_\xi = 1 + \frac{\sigma_\xi}{j\omega\varepsilon_0}$ ,  $\xi = x, y, z$ . From (1) and (2), we could get the modified

equation which can be utilized to derive the time domain formulation:

$$\begin{aligned} & \nabla \times \frac{1}{\mu} \nabla \times E + \frac{2}{j\omega\varepsilon_0} \nabla \times \frac{1}{\mu} [I] \nabla \times E - \frac{1}{\omega^2 \varepsilon_0^2} \nabla \times \frac{1}{\mu} [I]^2 \nabla \times E \\ & = \omega^2 \varepsilon E + \frac{2\omega\varepsilon}{j\varepsilon_0} [J] E - \frac{\varepsilon}{\varepsilon_0^2} ([J]^2 + 2[k]) E - \frac{2\varepsilon}{j\omega\varepsilon_0^3} [L] E + \frac{\varepsilon}{\omega^2 \varepsilon_0^4} [K]^2 E \end{aligned} \quad (3)$$

where

$$\begin{aligned} [I] &= \begin{bmatrix} \sigma_x & & \\ & \sigma_y & \\ & & \sigma_z \end{bmatrix}, [J] = \begin{bmatrix} \sigma_y + \sigma_z & & \\ & \sigma_z + \sigma_x & \\ & & \sigma_x + \sigma_y \end{bmatrix}, [K] = \begin{bmatrix} \sigma_y \sigma_z & & \\ & \sigma_z \sigma_x & \\ & & \sigma_x \sigma_y \end{bmatrix}, \\ [L] &= \begin{bmatrix} (\sigma_y + \sigma_z) \sigma_y \sigma_z & & \\ & (\sigma_z + \sigma_x) \sigma_z \sigma_x & \\ & & (\sigma_x + \sigma_y) \sigma_x \sigma_y \end{bmatrix}. \end{aligned} \quad (4)$$

Using the following transformation:

$$j\omega \leftrightarrow \frac{\partial}{\partial t}, -\omega^2 \leftrightarrow \frac{\partial^2}{\partial t^2}, \frac{1}{j\omega} \leftrightarrow \int_0^t, \frac{-1}{\omega^2} \leftrightarrow \int_0^t \int_0^t \quad (5)$$

We could recast equation (3) in the following form:

$$\begin{aligned} & \nabla \times \frac{1}{\mu} \nabla \times E + \frac{2}{\varepsilon_0} \nabla \times \frac{1}{\mu} [I] \int_t \nabla \times E + \frac{1}{\varepsilon_0^2} \nabla \times \frac{1}{\mu} [I]^2 \iint_t \nabla \times E \\ & = -\varepsilon \frac{\partial^2 E}{\partial t^2} - \frac{2\varepsilon}{\varepsilon_0} [J] \frac{\partial E}{\partial t} - \frac{\varepsilon}{\varepsilon_0^2} ([J]^2 + 2[k]) E - \frac{2\varepsilon}{\varepsilon_0^3} [L] \int_t E - \frac{\varepsilon}{\varepsilon_0^4} [K]^2 \iint_t E \end{aligned} \quad (6)$$

The electric fields are expanded using one-form Whitney edge elements  $W_i^{(1)}(\vec{r})$  ( $i = 1, 2, \dots, N$ ,  $N$  is the number of unknowns.) weighted by constant coefficients  $u_j$  that are continuous function of time [7].

$$\bar{E}(\bar{r}, t) = \sum_{j=1}^N W_j^{(1)}(\bar{r}) u_j(t) \quad (7)$$

Testing (6) with  $W_i^{(1)}(\bar{r})$ , associated with non-perfect-electric-conductor (PEC) edges of the grid, integrating by parts, equation (8) could be received.

$$[A]u + [B]\frac{du}{dt} + [C]\frac{d^2u}{dt^2} + [D]f + [E]g = 0 \quad (8)$$

Where

$$\begin{aligned} [A]_{ij} &= [S]_{ij} + [T_p]_{ij}, \quad [S]_{ij} = \int_V \frac{1}{\mu} \nabla \times W_i^{(1)} \cdot \nabla \times W_j^{(1)} dV, \\ [T_p]_{ij} &= \int_V \frac{\varepsilon}{\varepsilon_0^2} ([J]^2 + 2[K]) W_i^{(1)} \cdot W_j^{(1)} dV, \quad [B]_{ij} = [T_q]_{ij} = \int_V \frac{2\varepsilon}{\varepsilon_0} [J] W_i^{(1)} \cdot W_j^{(1)} dV, \\ [C]_{ij} &= [T]_{ij} = \varepsilon \int_V W_i^{(1)} \cdot W_j^{(1)} dV, \quad [D]_{ij} = \int_V \frac{2}{\mu \varepsilon_0} [I] \nabla \times W_i^{(1)} \cdot \nabla \times W_j^{(1)} + \frac{2\varepsilon}{\varepsilon_0^3} [L] W_i^{(1)} \cdot W_j^{(1)} dV, \\ [E]_{ij} &= \int_V \frac{1}{\mu \varepsilon_0^2} [I]^2 \nabla \times W_i^{(1)} \cdot \nabla \times W_j^{(1)} + \frac{\varepsilon}{\varepsilon_0^4} [K]^2 W_i^{(1)} \cdot W_j^{(1)} dV, \\ [S_1]_{ij} &= \int_V \frac{2}{\mu \varepsilon_0} [I] \nabla \times W_i^{(1)} \cdot \nabla \times W_j^{(1)} dV, \quad [Sth]_{ij} = \int_V \frac{1}{\mu \varepsilon_0^2} [I]^2 \nabla \times W_i^{(1)} \cdot \nabla \times W_j^{(1)} dV, \\ f &= \int_t u dt, \quad g = \iint_t u dt. \end{aligned} \quad (9)$$

By approximating the time derivatives with the Newmark-beta method, we have

$$\begin{aligned} (T + \Delta t^2 \beta S + \Delta t^2 \beta T_p + 0.5 \Delta t T_q) u^{n+1} &= (2T - \Delta t^2 (1 - 2\beta) S - \Delta t^2 (1 - 2\beta) T_p) u^n \\ &+ (-T - \Delta t^2 \beta S - \Delta t^2 \beta T_p + 0.5 \Delta t T_q) u^{n-1} \\ &- S_1 (\Delta t^2 \beta f^{n+1} + \Delta t^2 (1 - 2\beta) f^n + \Delta t^2 \beta f^{n-1}) \\ &- Sth (\Delta t^2 \beta g^{n+1} + \Delta t^2 (1 - 2\beta) g^n + \Delta t^2 \beta g^{n-1}) \end{aligned} \quad (10)$$

$$f^{n+1} = f^n + u^n \Delta t, \quad g^{n+1} = g^n + f^{n+1} \Delta t = g^n + f^n \Delta t + u^n \Delta t^2. \quad (11)$$

The choice of  $\beta \geq 0.25$  in the equation leads to an unconditionally stable scheme, allowing us to choose a time step for a specific accuracy without being constraint by stability requirements. Choosing  $\beta = 0.25$  minimized the solution error [8].

Equation (10) could also be rewritten in a matrix form as:

$$[C]X = [D] \quad (12)$$

In the 3-D case, (12) is often a large sparse linear system, which is very tedious and long to solve. Thus efficient methods to solve the system must be sought. Usually, the Krylov subspace iterative methods are used, among which the conjugate gradient algorithm (CG)

and the generalized minimal residue (GMRES) algorithm are most popular because they give monotonically decreasing error. The CG algorithm is only suitable for positive definite linear systems. When applied to indefinite systems, the following systems are to be solved:

$$[C]^H [C] X = [C]^H [D] \quad (13)$$

GMRES is to solve general non-symmetric and indefinite linear systems [37]. The convergence of conventional CG and GMRES is unacceptable slow for solving discretized Helmholtz equations. It is further desirable to precondition the coefficient matrix  $[C]$  so that the modified system can converge to an exact solution in significantly less iteration than its original counterpart. In this paper, different preconditioners are applied in combination with these two iterative algorithms to solve the large sparse equations in TDFEM.

The Jacobi preconditioner, which is the most simple and easiest preconditioner, is formed by the diagonal elements of the coefficient matrix [39-40]. However, its efficiency is often unsatisfied. The symmetric successive over relaxation (SSOR) [31, 33, 36, 39] preconditioner contains more global information of the coefficient matrix when compared with the Jacobi preconditioner. Therefore, the SSOR preconditioner can speed up the iterative algorithm more efficiently. The efficient SSOR preconditioning strategy deployed in this work follows the implementation described in [31]. The advantage of the Jacobi and SSOR preconditioners is that they can be directly derived from the coefficient matrix  $[C]$  without additional sacrifice.

Another kind of powerful preconditioner is the incomplete LU (ILU) factorization of the coefficient matrix and its variants. The simplest ILU preconditioner, *i.e.* the ILU(0) preconditioner which is used in this paper, is derived from ILU factorization without fill-in elements. Although additional computing time is required when forming the ILU preconditioners, the factorization need to be done only once before the first time step [38].

In the following of this paper, the convergence properties and CPU time used by preconditioned CG, GMRES and conventional CG, GMRES methods are compared and analyzed.

### III. NUMERICAL RESULTS AND DISCUSSIONS

In order to compare different convergence characteristics of the iterative methods in this work, a cylindrical cavity partially filled with dielectric rod, a partial-height dielectric-filled rectangular waveguide and waveguide inserted in cylindrical cavity structure are simulated. Numerical simulations are carried out by the TDFEM. And the large systems of the linear equations resulting from the TDFEM are solved by preconditioned CG, GMRES methods and also conventional CG and GMRES methods. The residual errors are defined as  $R = \|D - CX\| / \|D\|$  for the iterative algorithm and they are defined as  $10^{-6}$  for all of the algorithms and structures. All the examples are simulated on an Intel Pentium IV 2.4GHz PC with 512MB RAM.

A cylindrical cavity partially filled with a dielectric rod [23] is analyzed as the first

example in order to exploit the versatility of the TDFEM spatial discretization features. The relative permittivity of the dielectric rod and the dimensions of the structure are shown in Figure 1. A sinusoidal modulated Gaussian pulse of the following form is used as the excitation:

$$g(t) = e^{-\left(\frac{t-t_0}{T}\right)^2} \sin 2\pi f_0 (t-t_0) \quad (14)$$

Where  $T = 3.18 \times 10^{-10}$  s and  $t_0 = 3T$ . The central frequency is  $f_0 = 2.5$  GHz. The time step is  $\Delta t = 6.67 \times 10^{-12}$  s and  $N = 2^{15}$  for Fourier transformations. The number of tetrahedrons in the finite element region is equal to 3510, yielding 3540 unknowns.

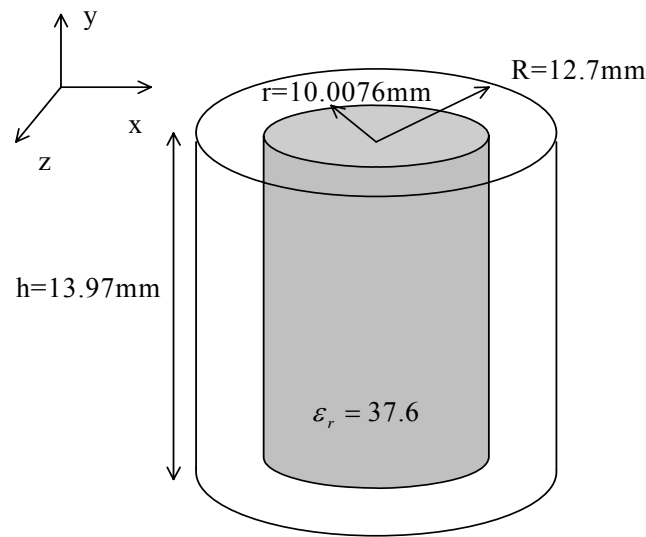


Figure 1 Cylindrical cavity partially filled with dielectric rod

Figure 2(a) displays the convergence characteristics of the Jacobi preconditioned, SSOR preconditioned, ILU0 preconditioned and conventional CG algorithms of the second time step. It can be found from Figure 2(a) that the ILU0-CG method converges in the fastest way. Figure 2(b) displays the convergence characteristics of the Jacobi preconditioned, SSOR preconditioned, ILU0 preconditioned and conventional GMRES algorithms, again for the second time step. It also can be found from Figure 2(b) that the ILU0-GMRES method converges in the fastest way. Table I presents the time used for the first 100 time steps for all of the algorithms. We could find that the ILU0 preconditioning strategy cost the smallest time for both the preconditioned CG and GMRES methods.

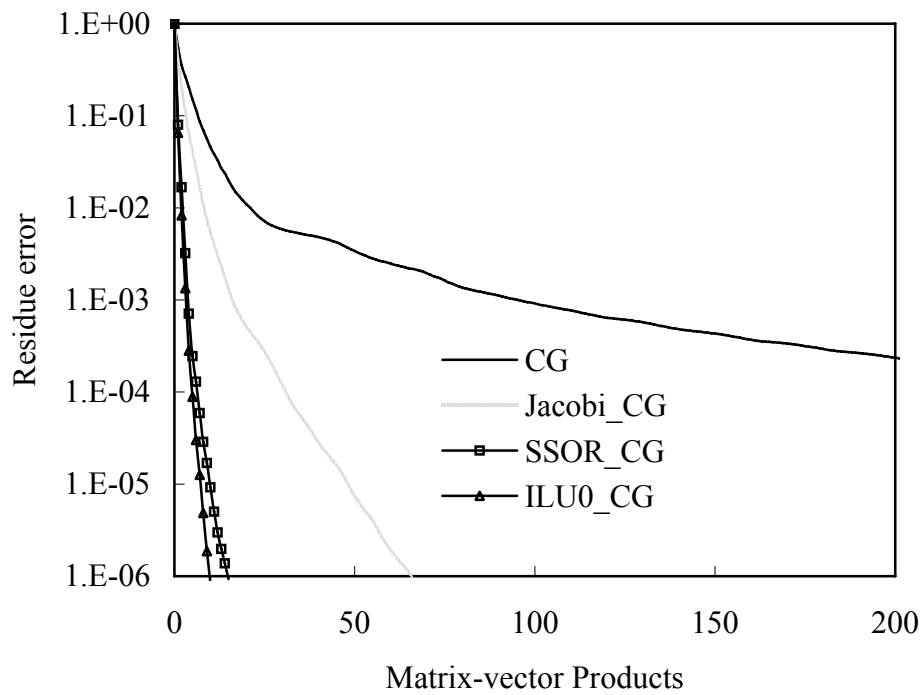


Figure 2(a) Residue errors versus iteration number for CG, Jacobi\_CG, SSOR\_CG and ILU0\_CG methods for the second time step

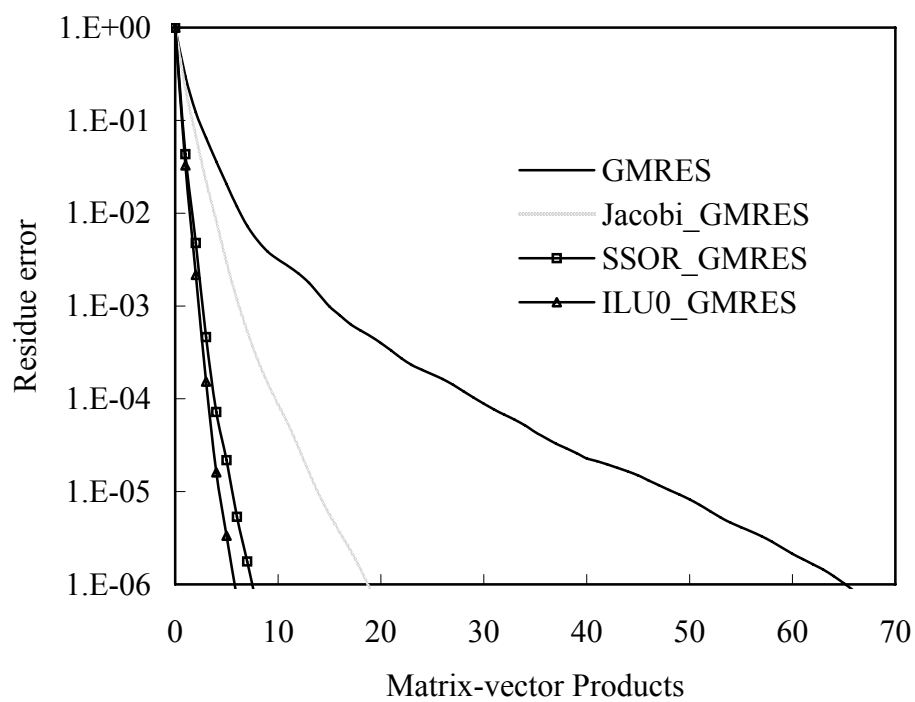


Figure 2(b) Residue errors versus iteration number for GMRES, Jacobi\_GMRES, SSOR\_GMRES and ILU0\_GMRES methods for the second time step

Table I Total time of the first 100 time steps for CG, Preconditioned CG, GMRES, and Preconditioned GMRES

	No Precondition	Jacobi	SSOR	ILU0
CG	3051 s	273 s	107 s	103 s
GMRES	400 s	93 s	42 s	39 s

Figure 3(a) shows the y-component of the electric field at the observation point (5.0038, 6.985, -5.0038) mm, the normalized spectral amplitude of which is shown in Figure 3(b). The resonant frequencies, corresponding to spectral peaks are clearly detected. Table II compares four resonant frequencies of the partially filled cylindrical cavity received by TDFEM method with those analytical values [24]. Very good agreements are obtained and the relative error of each resonant frequency is under 1%.

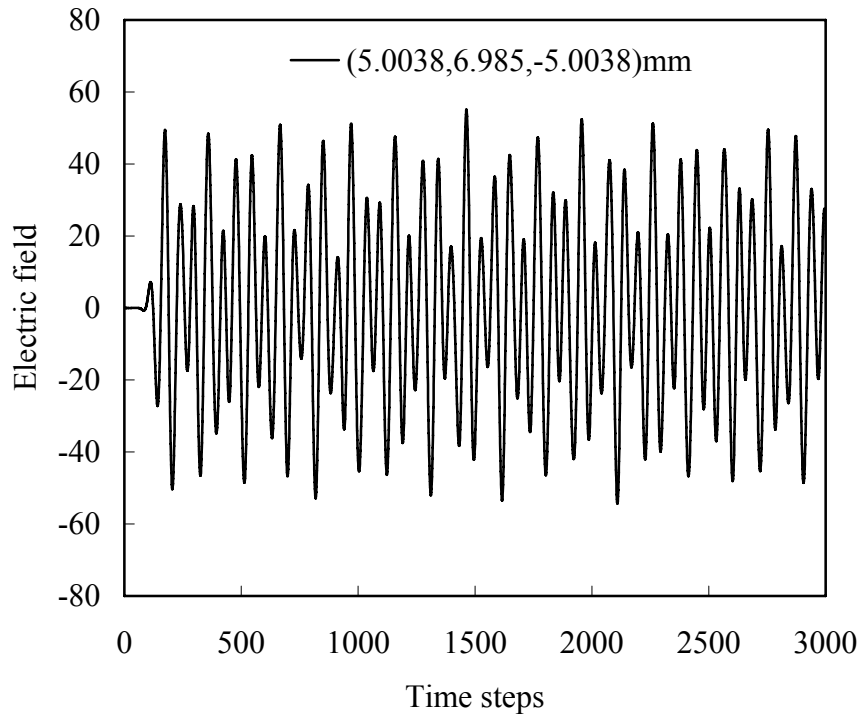


Figure 3(a) y-component of the electric field at the observation point (5.0038, 6.985, -5.0038) mm



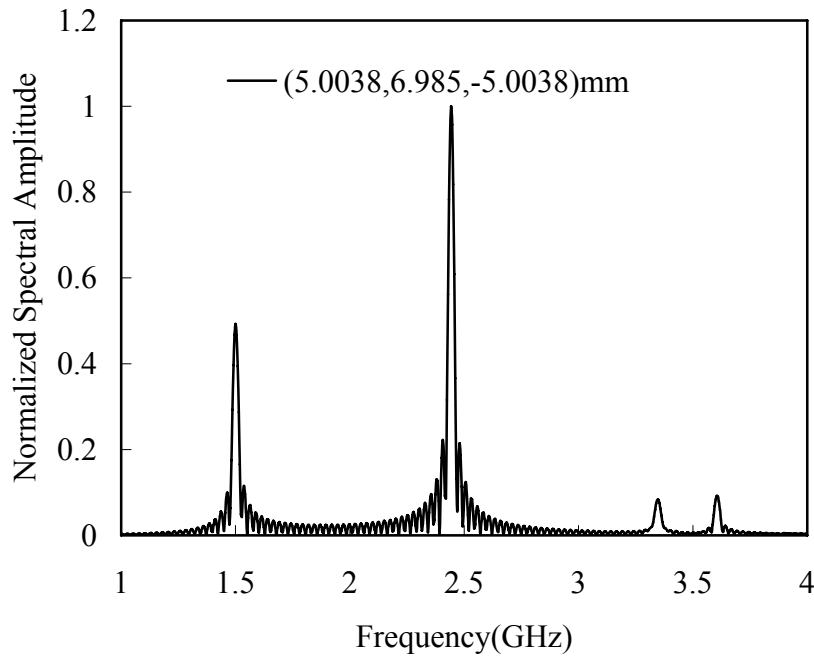


Figure 3(b) Normalized spectral amplitude of the electric field at the observation point (5.0038, 6.985, -5.0038) mm

Table II Four resonant frequencies of the partially filled cylindrical cavity

Resonant frequency (GHz)		Relative error (%)
Analytical results [24]	TDFEM	
1.498	1.50043	0.16
2.435	2.44277	0.32
3.339	3.34851	0.28
3.596	3.60468	0.24

In order to investigate the adaptability of the priority of the ILU0 preconditioning strategy to different microwave structures, the preconditioned GMRES methods are applied to PML terminated waveguide structures. The application of PML absorbers within computational domain will deteriorates the condition number of the TDFEM system matrix [31] and makes iterative solvers take more iteration to reach convergence.

The second example is the waveguide structure partially filled with a dielectric [31] as shown in Figure 10. The rectangular waveguide has the width of  $a = 20\text{mm}$  and a height of  $b = 10\text{mm}$ . The inserted dielectric material slab has a dimension of  $c = 8.88\text{mm}$ ,  $W = 8\text{mm}$ ,  $d = 3.99\text{mm}$  and a dielectric constant of  $\varepsilon_r = 6$ . A sinusoidal modulated Gaussian pulse with central frequency of 10GHz is used as the excitation source. Magnetic wall on the plane  $x = \max x$  is used and half of the structure needs to be simulated. The waveguide is terminated with PML medium backed with a perfect conductor. The number of tetrahedrons in the finite element region is equal to 18000, yielding 19698 unknowns. In all computations we used  $\Delta t = 1.667\text{ps}$ .

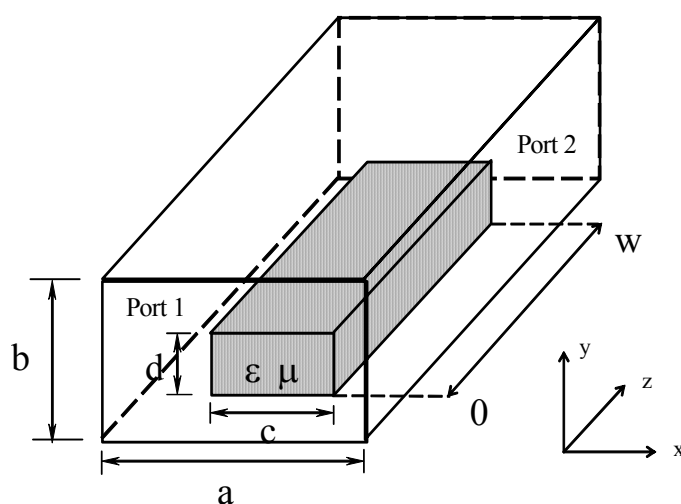


Figure 4 Configuration of partial-height dielectric-filled rectangular waveguide

Figure 5 displays the convergence characteristics of the Jacobi preconditioned, SSOR preconditioned, ILU0 preconditioned and conventional GMRES algorithms, which are applied to the waveguide structure, for the second time step. Table III presents the time used for the first 50 time steps for all of the algorithms. As the time steps increases, much more time could be saved when using ILU0-GMRES method. It can be found that the ILU0-GMRES method converges in the fastest way.

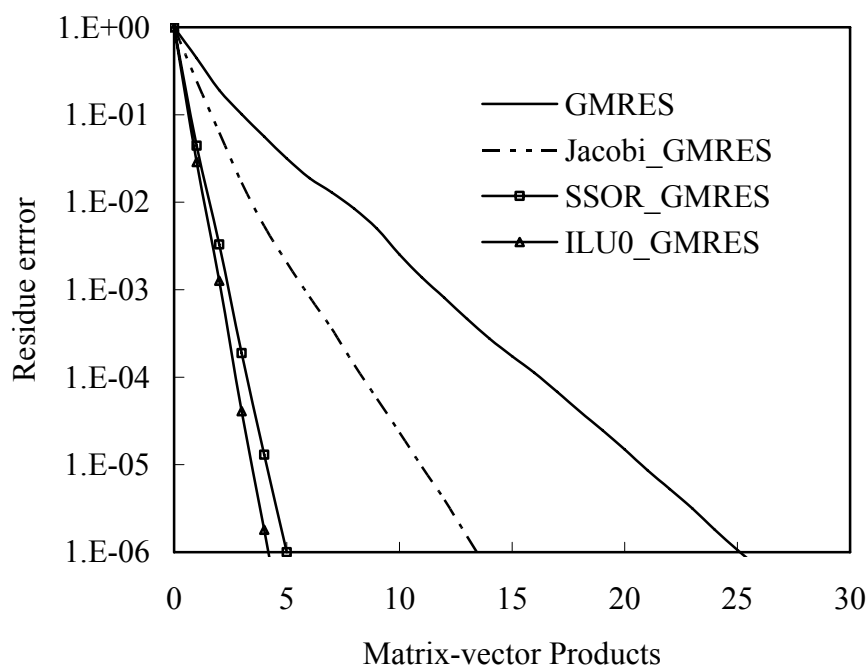


Figure 5 Residue errors versus iteration number for GMRES, Jacobi\_GMRES, SSOR\_GMRES and ILU0\_GMRES methods for the second time step

Table III Total time of the first 50 time steps for GMRES, and Preconditioned GMRES

	No Precondition	Jacobi	SSOR	ILU0
GMRES	434 s	165 s	102 s	99 s

Figure 6(a) plots the time domain voltage waveforms at the observation point in Ports 1. The waveform of  $v_l$  shown in Figure 6(a) is the incident voltage obtained by a separate pre-simulation when the dielectric is absent. The  $S_{11}$  parameter is calculated and shown in Figure 6(b). Simulation results obtained by the TDFEM are in good agreement with that of the frequency domain FEM algorithm.

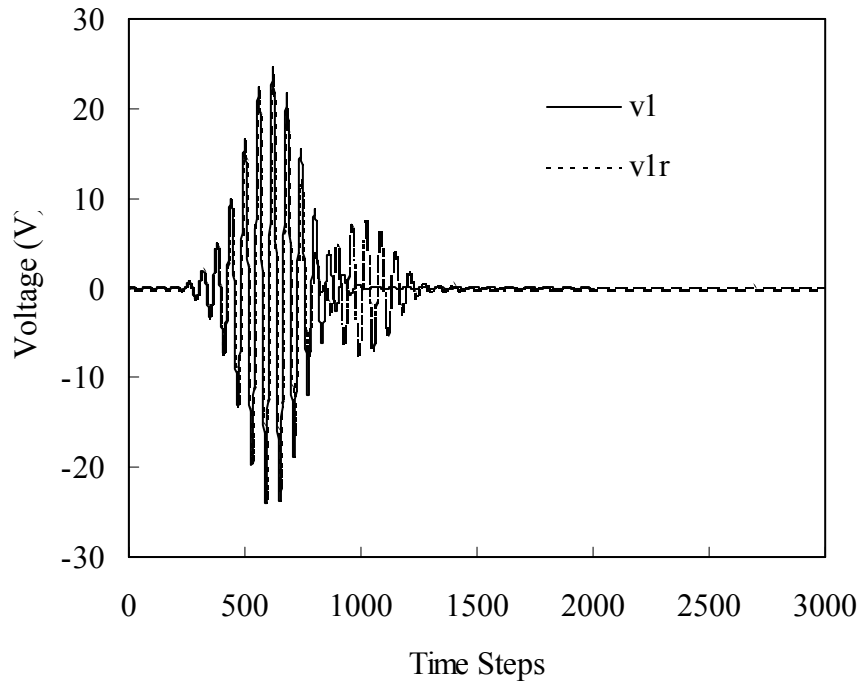


Figure 6(a) Time domain voltage waveforms at the observation points in Ports 1,  $v_l$  is the incident voltage obtained by a separate pre-simulation when the dielectric is absent

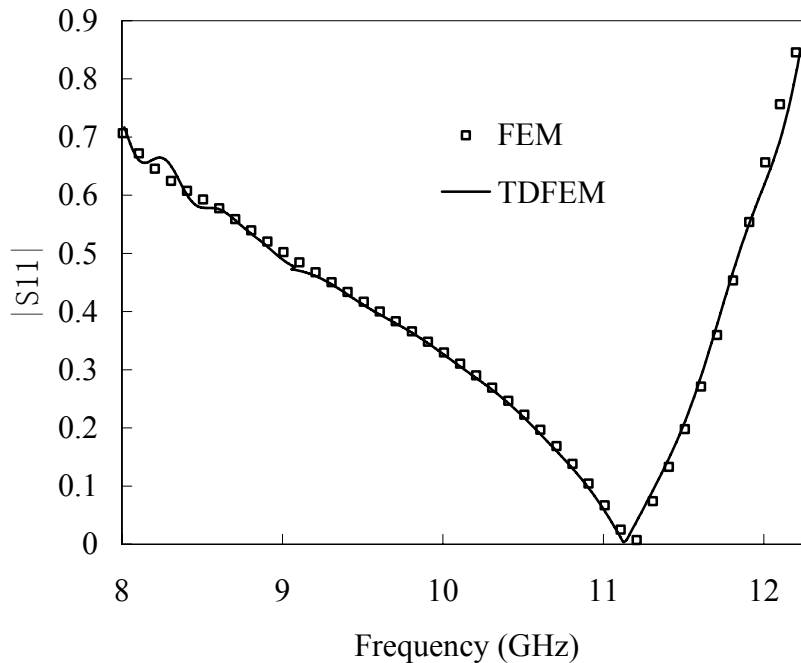


Figure 6(b) Magnitude of  $S_{11}$  versus frequency for the dielectric-filled rectangular waveguide

The third example is a waveguide inserted in cylindrical cavity structure [41], as shown in Figure 7. This kind of structure can be applied to design high quality filter. The height  $b$  of the rectangular waveguide is equal to the height  $h$  of the cylindrical cavity with  $b = h = 7.9mm$  and also the width of the waveguide is equal to the radius of the cylindrical cavity with  $a = R = 15.8mm$ . A sinusoidally modulated Gaussian pulse with central frequency of 15GHz is used as the excitation source. The structure is terminated with PML medium backed with a perfect conductor. The number of tetrahedrons in the finite element region is equal to 24243, yielding 23944 unknowns. In all computations we used  $\Delta t = 0.667ps$ .

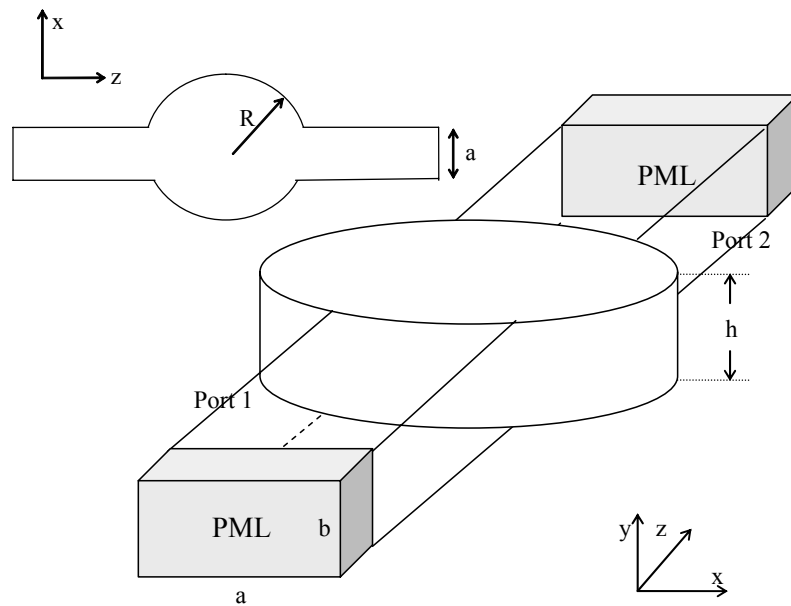


Figure 7 The waveguide inserted in cylindrical cavity structure

Figure 8 displays the convergence characteristics of the Jacobi preconditioned, SSOR preconditioned, ILU0 preconditioned and conventional GMRES algorithms, which are applied to this waveguide inserted in cylindrical cavity structure, for the second time step. Table IV presents the time used for the first 100 time steps for all of the algorithms. As the time steps increases, much more time could be saved when using ILU0-GMRES method. It can be found that the ILU0-GMRES method converges in the fastest way.

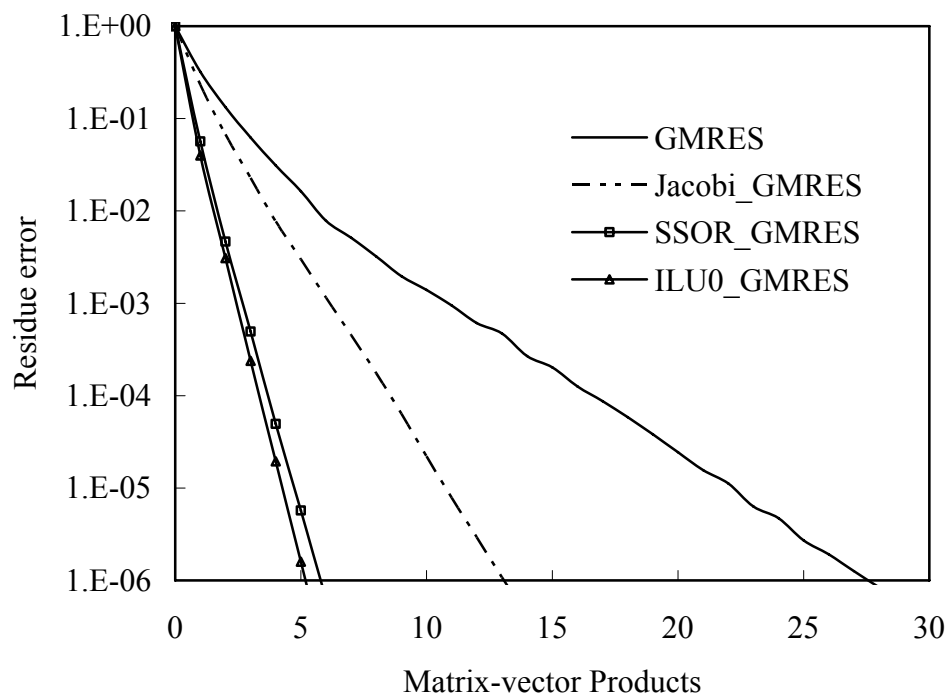


Figure 8 Residue errors versus iteration number for GMRES, Jacobi\_GMRES, SSOR\_GMRES and ILU0\_GMRES methods for the second time step

Table IV Total time of the first 100 time steps for GMRES, and Preconditioned GMRES

	No Preconditioning	Jacobi	SSOR	ILU0
GMRES	1226 s	385 s	288 s	248 s

Figure 9(a) plots the time domain voltage waveforms at the observation points in Ports 1 and 2. Based on these time domain data, the scattering parameters are calculated and shown in Figure 9(b). Simulation results obtained by the TDFEM are in good agreement with those of the frequency domain FEM algorithm.

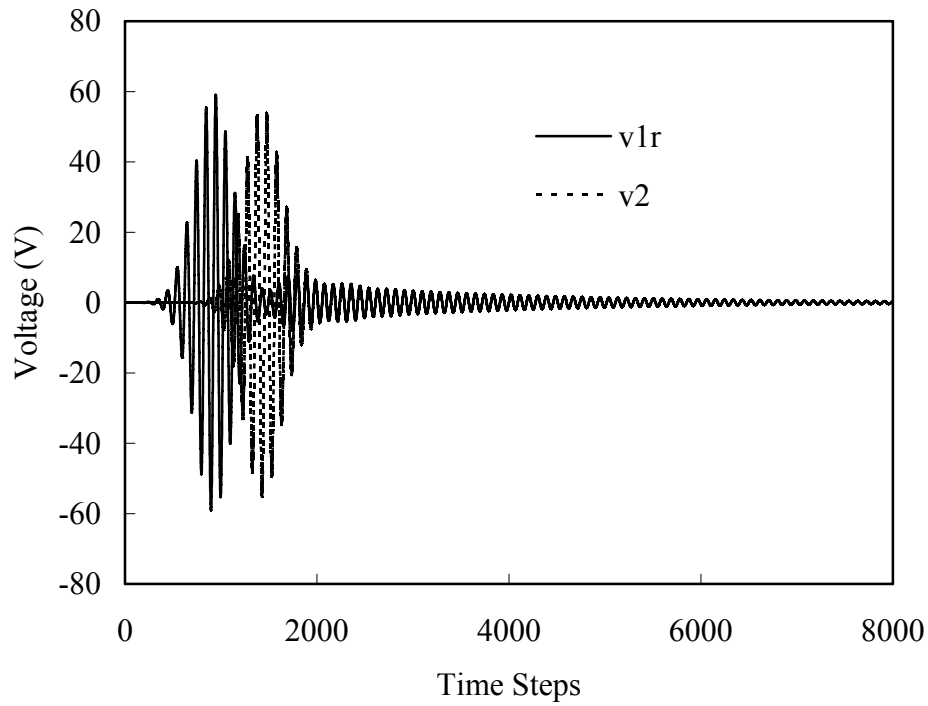


Figure 9(a) Time domain voltage waveforms at the observation points in Ports 1 and 2

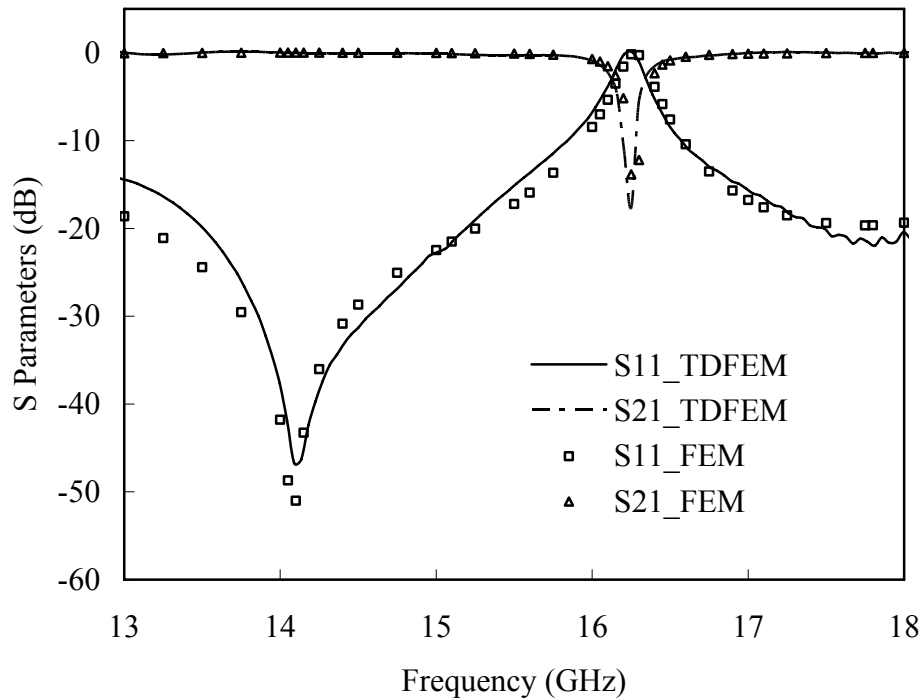


Figure 9(b) Scattering parameters of the waveguide inserted in cylindrical cavity structure

#### IV. CONCLUSIONS

The iterative methods are used to solve the large system of linear equations resulted from the time-domain finite element methods (TDFEM). Several preconditioning techniques, such as Jacobi、SSOR and ILU0, are used to accelerate the convergence of

iterative methods, such as CG and GMRES. Convergence properties and the time used of these conventional preconditioning techniques are also compared and analyzed. Cylindrical cavity partially filled with dielectric rod and the waveguide structures are simulated. Numerical results show that the ILU0 preconditioned method converges the fastest and costs the smallest time in TDFEM when compared with other preconditioning techniques computing the same number of time steps. We get the conclusion that the ILU0 preconditioning strategy is especially effective for iterative methods when the TDFEM is applied to analyze the electromagnetic-field problems.

## V. ACKNOWLEDGMENTS

This work is supported partially by JiangSu Natural Science Foundation under contract number BK2006203, Natural Science Foundation of China under Contract number 60431010 and 60701004, Excellent Youth Natural Science Foundation of China under Contract number 60325103 and Doctoral Creation Foundation of Nanjing University of Science and Technology, China.

## VI. REFERENCES

- [1] A. Taflove, Computational Electrodynamics: The Finite Difference Time Domain Method, second edition. Norwood, MA: Artech House, 2000.
- [2] R. S. Chen, Z. B. Ye, Edward K. N. Yung, "A new Ka-band microstrip Y-junction circulator with a ferrite sphere," International Journal of Electronics 90 (2003), 121-132.
- [3] R. S. Chen, Z. B. Ye, Edward K. N. Yung, "CAD of millimeter wave Y-junction circulators with a ferrite sphere," International Journal of Infrared and Millimeter Waves 24 (2003) 1325-1339.
- [4] Y. Yang, R. S. Chen, "Analysis of Planar Circuits Using Unconditionally Stable Three-Dimensional ADI-FDTD Method," Microwave and Optical Technology Letters 46 (2005), 175-179.
- [5] Y. Yang, R. S. Chen, "Efficient ADI-FDTD/Modified Matrix Pencil Method for the Microwave Integrated Circuits Analysis," Microwave and Optical Technology Letters 46 (2005), 391-395.
- [6] Y. Yang, R.S. Chen, D.X. Wang and Edward K.N. Yung, "Unconditionally Stable Crank–Nicolson Finite-Difference Time-Domain Method for Simulation of 3-D Microwave Circuits," IEE Proc.-Microw. Antennas Propag. 1 (2007), 937-942.
- [7] J. F. Lee, "WETD-A Finite Element Time-Domain Approach for Solving Maxwell's Equations," IEEE Microwave and Guided wave letters 4 (1994), 11–13.
- [8] Stephen D. Gedney, Umesh Navsariwala, "An Unconditionally Stable Finite Element Time-Domain Solution of the Vector Wave Equation," IEEE Microwave and Guided wave letters 5 (1995), 332-334.
- [9] J. F. Lee, R. Lee, and A. Cangellaris, "Time-domain finite-element methods," IEEE Trans. Antennas Propagat. 45 (1997) 430–442.
- [10] Hsiao-Ping Tsai, Yuanxun Wang, Tatsuo Itoh, "An Unconditionally Stable Extended (USE) Finite-Element Time-Domain Solution of Active Nonlinear Microwave

- Circuits Using Perfectly Matched Layers,” IEEE Tran. Microwave Theory Tech. 50 (2002), 2226-2232.
- [11] D. Jiao and J. M. Jin, Eric Michielssen and Douglas J. Riley, “Time-Domain Finite-Element Simulation of Three-Dimensional Scattering and Radiation Problems Using Perfectly Matched Layers,” IEEE Trans. Antennas Propagat. 51 (2003), 296-305.
- [12] J. M. Jin, The Finite Element Method in Electromagnetics, second edition. New York: Wiley, 2002.
- [13] Man-Fai Wong, Odile Picon and Victor Fouad Hanna, “A Finite Element Method Based on Whitney Forms to Solve Maxwell Equations in the Time Domain,” IEEE Transactions on magnetics 31 (1995), 1617-1621.
- [14] Bo He, F.L. Teixeira, “Geometric finite element discretization of Maxwell Equations in primal and dual spaces,” Physics Letters A 349 (2006), 1-14.
- [15] Masoud Movahhedi, Abdolali Abdipour, “Optimization of the Perfectly Matched Layer for the Finite-Element Time-Domain Method,” IEEE microwave and wireless components letters 17 (2007), 10-12.
- [16] Masoud Movahhedi, Abdolali Abdipour, “Alternation-Direction Implicit Formulation of the Finite-Element Time-Domain Method,” IEEE Tran. Microwave Theory Tech. 55 (2007), 1322-1331.
- [17] Salah Benhassine, Walter P. Carpes, Jr., and Lionel Pichon, “Comparison of Mass lumping Techniques for solving the 3D Maxwell’s Equations in the Time Domain,” IEEE Transactions on magnetics 36 (2000), 1548-1552.
- [18] Bo He, F.L. Teixeira, “Sparse and Explicit FETD via Approximate Inverse Hodge (Mass) Matrix,” IEEE microwave and wireless components letters 16 (2006), 348-350.
- [19] Daniel A. White, “Orthogonal vector basis functions for time domain finite element solution of the vector wave equation”, IEEE Transactions on magnetics 35 (1999), 1458-1461.
- [20] D. Jiao, Jian-Ming Jin, “Three-Dimensional Orthogonal Vector Basis Functions for Time-Domain Finite Element Solution of Vector Wave Equations.” IEEE Trans. Antennas Propagat. 51 (2003), 59-66.
- [21] Zheng Lou, Jian-Ming Jin, “A Novel Dual-Field Time-Domain Finite-Element Domain-Decomposition Method for Computational Electromagnetics,” IEEE Trans. Antennas Propagat. 54 (2006), 1850-1862.
- [22] Zheng Lou, Jian-Ming Jin, “A new explicit time-domain finite-element method based on element-level decomposition,” IEEE Trans. Antennas Propagat. 54 (2006), 2990-2999.
- [23] W.P.Carpes Jn, L.Pichon and A.Razek, “Efficient analysis of resonant cavities by finite element method in the time domain,” IEE Proc.-Microw. Antennas Propag. 147 (2000), 53-56.
- [24] Mahadevan K., Mittra R., Vaidya P.M., “Use of Whitney’s edge and face elements for finite time domain solution of Maxwell’s equations,” Journal of electromagnetic waves and applications 8 (1994), 1173 - 1191.
- [25] R.S.Chen, D.X.Wang, Edward K.N.Yung, and J.M.Jin “ A Fast Analysis of Microwave Devices by the Combined Unifrontal/ Multifrontal Solver for



- Unsymmetric Sparse Matrices”, Microwave and Optical Technology Letters 35 (2002), 76-81.
- [26] R.S.Chen, Z.H.Qian, and Edward K.N.Yung, “Simulation of Millimeter Wave Circulators by FEM with Unifrontal /Multifrontal Technique”, International Journal of Infrared and Millimeter Waves 23 (2002), 873-889.
- [27] R.S.Chen, Edward.K.N.Yung, C.H.Chan, D.G.Fang, "Application of preconditioned conjugate gradient method to edge-FEM for Electromagnetic problems", Microwave and Optical Technology Letters 27 (2000), 235-238.
- [28] R.S.Chen, K.F.Tsang, L.Mo, “Wavelet Based Sparse Approximate Inverse Preconditioned CG Algorithm for Fast Analysis of Microstrip Circuits”, Microwave and Optical Technology Letters 35 (2002), 383-389.
- [29] R.S.Chen, Edward K N Yung, C.H.Chan, D.X.Wang, and J.M.Jin, “An Algebraic Domain Decomposition Algorithm for the Vector Finite Element Analysis of 3D Electromagnetic Field Problems”, Microwave and Optical Technology Letters 34 (2002), 414-417.
- [30] R.S.Chen, Edward K.N.Yung, A.H.Yang, and C.H.Chan, “Application of preconditioned Krylov subspace iterative FFT techniques to Method of Lines for analysis of the infinite plane metallic grating”, Microwave and Optical Technology Letters 35 (2002), 160-167.
- [31] R. S. Chen, E. K. N. Yung, C. H. Chan, D. X. Wang, and D. G. Fang, “Application of the SSOR Preconditioned CG Algorithm to the Vector FEM for 3-D Full-Wave Analysis of Electromagnetic-Field Boundary-Value Problems,” IEEE Trans. Microwave Theory Tech. 50 (2002), 1165-1172.
- [32] R.S. Chen, X.W. Ping, Edward K.N. Yung, C.H. Chan etc, “Application of Diagonally Perturbed Incomplete Factorization Preconditioned Conjugate Gradient Algorithms for Edge Finite Element Analysis of Helmholtz Equations,” IEEE Trans. Antennas Propagat. 54 (2006), 1604-1608.
- [33] R.S. Chen, L. Yang, L. Zhao, Y.M. Siu and K.K. Soo, “SSOR preconditioned CG method for the linear interference cancellation of asynchronous CDMA systems”, International Journal of Electronics 91 (2004), 745-757.
- [34] R.S. Chen, L. Yang, Y.M. Siu, L. Zhao and K.K. Soo, “Linear Interference Cancellation of Asynchronous CDMA Systems by Preconditioned CG Method”, Journal of Wireless Personal Communications 31 (2004), 51-62.
- [35] R.S.Chen, D.X.Wang, Edward K.N.Yung, “Efficient Analysis of Millimeter Wave Ferrite Circulators by GMRES Iterative Algorithm,” International Journal of Infrared and Millimeter Waves 24 (2003), 1199-1214.
- [36] R. S. Chen, X. W. Ping, D. X. Wang, Edward K.N.Yung, “SSOR preconditioned GMRES for the FEM analysis of waveguide discontinuities with anisotropic dielectric,” International Journal of Numerical Modeling: Electronic Networks, Devices and Fields 17 (2004), 105-118.
- [37] Y. Saad and M. Schultz. GMRES: A generalized minimal residual algorithm for solving nonsymmetric linear systems. SIAM J. Sci. Stat. Comput. 7 (1986), 856-869.
- [38] Y. Saad, Iterative methods for sparse linear systems. Boston: PWS publishing company, 1998.
- [39] R.S.Chen, K.F.Tsang, Edward K.N.Yung “Application of SSOR Preconditioning

Technique to Method of Lines for Millimeter Wave Scattering”, International Journal of Infrared and Millimeter Waves 21 (2000), 1281-1301.

- [40] R.S.Chen, Edward K.N.Yung, C.H.Chan and D.G.Fang, “Application of preconditioned CG-FFT technique to method of lines for analysis of the infinite plane metallic grating”, Microwave and Optical Technology Letters 24 (2000), 170-175.
- [41] Zhenyu Ding, Wei Hong, “S-Parameters of Waveguide Inserted in Cylindrical Cavity Structure,” Journal of Southeast University 30 (2000), 42-46.